RSC Medicinal Chemistry

ROYAL SOCIETY OF CHEMISTRY

RESEARCH ARTICLE

View Article Online
View Journal | View Issue

Cite this: *RSC Med. Chem.*, 2025, **16**, 3736

N-Heterocyclic carbene platinum complexes encapsulated in lipid particles: a novel strategy to target cancer cells and cancer stem cells in glioblastoma†

Patricia Fernandez de Larrinoa, [ab] Antoine Kichler, [b] Monique Dontenwill, [c] Christel Herold-Mende, [d] Sylvie Fournel, [b] Benoît Frisch, [b] Stéphane Bellemin-Laponnaz *[a] and Béatrice Heurtault *[b]

The properties against cancer cells and glioblastoma stem cells of a series of platinum NHC complexes in lipid formulations are reported. As these organometallic compounds show very promising biological activities using conventional formulations, *i.e.* by solubilization in a DMSO/water system, the challenge for a therapeutic application is to be able to make them biocompatible while retaining this activity. Herein with the aim of eradicating cancer cells and cancer stem cells from glioblastoma, a disease in need of new therapies, we studied the encapsulation of platinum compounds in either liposome or lipid nanocapsule formulations and investigated the physical and chemical stability of the resulting nano-objects. It was then demonstrated that in these lipid formulations, platinum complexes retained their cytotoxic activity on both cancer cells and cancer stem cells. The best candidate, *i.e.* triphenylphosphonium-functionalized platinum-based complex, was then used for *in vivo* studies on mice using a U87-MG glioblastoma model, with significant results in slowing tumor growth, in particular when comparing to oxaliplatin. Another key strength of this study is the preservation of the compound's anti-cancer activity within a lipid-based formulation, eliminating the need for DMSO as a solvent. The findings of this study signify a major advance in the field, particularly in light of the expanding body of research on organometallic complexes conducted under conditions that preclude direct clinical applicability.

Received 21st May 2025,
Accepted 1st June 2025

DOI: 10.1039/d5md00460h

rsc.li/medchem

Introduction

Glioblastoma is a highly aggressive brain cancer most often diagnosed in adults with significant medical complications. Current treatments include surgical resection followed by a combination of radiotherapy and temozolomide chemotherapy. However, the effectiveness of this therapy is hampered by the development of drug resistance and non-specific toxicity.[1,2] To overcome limitations, various encapsulation strategies have been investigated, including the use of polymer-based and lipid-based systems as well as other materials.[3,4] Furthermore, cancer stem cells (CSCs) play an important role in therapeutic resistance and tumour recurrence in a variety of cancers, including glioblastoma. Therefore, in addition to killing cancer cells, eradication of CSCs is crucial for an effective and definitive treatment,[5–8] a task which is not achieved with temolozomide.[9]

Platinum derivatives are widely used in chemotherapy, with cisplatin being the main drug for the treatment of various cancers such as ovarian, uterine, lung, testicular and bladder cancers.[10] Another commonly used platinum derivative, oxaliplatin, is effective against metastatic colorectal, colon, pancreas and stomach cancers.[11] However, these alkylating drugs, which act by damaging nuclear DNA, are associated with severe systemic toxicity and resistance phenomena.[12–15] A substantial body of research has been dedicated to the study of platinum-based drugs as a potential treatment for glioblastoma. However, they have demonstrated minimal efficacy, often accompanied by significant toxicity to

[a] *Institut de Physique et Chimie des Matériaux de Strasbourg (IPCMS), UMR7504, Université de Strasbourg & CNRS, 23 Rue du Loess, F-67083 Strasbourg, France. E-mail: bellemin@unistra.fr*
[b] *Institut national de la Recherche Médicale (INSERM), Centre National de la Recherche Scientifique (CNRS), Biomaterials and Bioengineering, UMR_S 1121 INSERM/EMR 7003 CNRS, Faculté de Pharmacie, Université de Strasbourg, Illkirch, France. E-mail: bheurtault@unistra.fr*
[c] *Faculté de Pharmacie, UMR7021 Université de Strasbourg & CNRS, 74 route de Rhin, 67401 Illkirch Cedex, France*
[d] *University Hospital Heidelberg, Department of Neurosurgery, Division of Neurosurgical Research, Neuenheimer Feld 400, 69120 Heidelberg, Germany*

† Electronic supplementary information (ESI) available. CCDC 2373163. For ESI and crystallographic data in CIF or other electronic format see DOI: **https://doi.org/10.1039/d5md00460h**

the central nervous system.[16] Nevertheless, the development of innovative administration strategies that can mitigate toxicities has the potential to redirect the utilization of this class of chemotherapeutic drugs in the treatment of glioblastoma.[17–19] The need to develop new and more suitable platinum-based anti-tumoral compounds, particularly in the context of glioblastoma, remains valid.[20]

This last decade, the use of *N*-heterocyclic carbene (NHC) ligands to stabilize metals has proven to be a promising strategy to develop effective cancer therapy.[21–27] Platinum NHC (NHC-Pt) complexes but also other metal NHC complexes, particularly gold and silver,[28–30] have been extensively investigated as potential metallodrugs.[31–39] Compared with conventional platinum molecules, these NHC complexes usually offer high stability, easy functionalization, and enhanced cytotoxicity, with seemingly different modes of action.[9,40–44] We have recently shown that NHC-Pt complexes accumulate efficiently in mitochondria[40] and that the introduction of a pendant triphenylphosphonium group on the NHC ligand leads to increased targeting of this organelle and increases the production of reactive oxygen species. It was also observed that CSCs were killed more efficiently than differentiated glioblastoma cells,[45] a result that could be correlated with a higher dependence on mitochondrial biogenesis for survival and proliferation in cancer stem cells.[43,44,46,47]

Despite the great progress that has been made, there is still a long way to go before these compounds reach the clinic. With a few exceptions,[39,44] the poor solubility of NHC-Pt complexes in water necessitates the use of organic solvents such as dimethyl sulfoxide (DMSO) to ensure the maintenance of biological activity, which renders them unsuitable for clinical applications.[48–51] Concerning all NHC metallic complexes, only silver, gold, and iridium complexes have undergone encapsulation for biological applications.[52–55] On the other hand, it is interesting to note that some conventional platinum drugs have been encapsulated for improving drug stability and solubility, reducing toxic effects and improving therapeutic outcomes.[56,57]

In this work, the primary objective was to address the solubilization challenge of NHC-Pt complexes in water to avoid the use of DMSO and other organic solvents. Two lipid-based delivery systems were investigated, characterized and compared, namely liposomes and lipid nanocapsules (LNCs). Remarkably, each NHC-Pt derivative tested demonstrated successful nanoencapsulation, a notable innovation which had not been accomplished previously. Furthermore, it has been observed that the chemical stability of the platinum complex can pose a challenge during the encapsulation process. Finally, *in vitro* studies on glioblastoma cancer cell lines as well as on glioblastoma cancer stem cells revealed that cytotoxicity was maintained after encapsulation and preliminary *in vivo* assays in a tumor mouse model were performed. This approach opens up new avenues for advancing the application of NHC-Pt compounds in biomedical research and potential therapeutic interventions.

Results

Synthesis and stability of NHC platinum complexes

We previously identified various NHC platinum complexes that proved efficient for killing cancer cells and cancer stem cells. Among all the compounds that had demonstrated interesting cytotoxicity, we chose three NHC platinum candidates whose characteristics we felt were appropriate for formulation either with liposomes or lipid nanocapsules, namely complexes **1**, **2** and **3** (Fig. 1).[45,58,59] Compounds **1** and **2** are neutral Pt complexes whereas compound **3** displays a cationic mitochondria-targeting triphenylphosphonium moiety. It is worth mentioning that while compound **3** has demonstrated a considerable production of reactive oxygen species within mitochondria in glioblastoma cancer stem cells (NCH421K),[45] complex **2** was remarkably efficient on various cancer cell lines.[58]

Complexes **1** and **2** were synthesized following the classical method, using excesses of KI and K_2CO_3, $PtCl_2$ and pyridine as a solvent at 100 °C.[60] The synthesis of complex **3** requires gentle experimental conditions to avoid decomposition of the carbene ligand precursor. Therefore, the synthesis may be accessible starting from the $PtCl_2(SMe_2)$ precursor, which reacts with the free carbene generated *in situ* at room temperature.[61] All complexes were easily purified by chromatography on silica gel and display high stability with air and moisture. As usual for this type of complex, these compounds are soluble in all

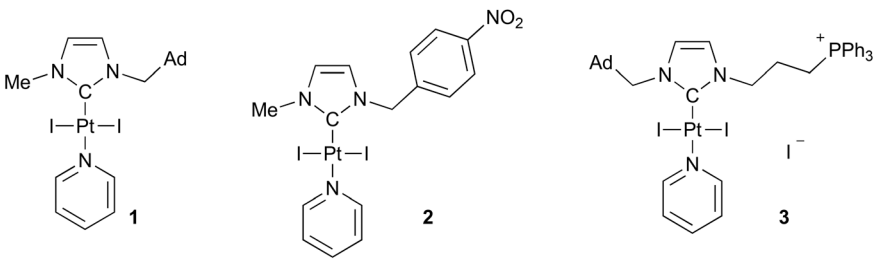

Fig. 1 Molecular structure of the synthesized NHC platinum complexes **1**–**3**. Complexes **1** and **2** were obtained in a one-step procedure from the corresponding imidazolium, $PtCl_2$, KI, and K_2CO_3 in pyridine (100 °C). Complex **3** was obtained in two steps starting from imidazolium, $PtCl_2(SMe_2)$, KI, and K_2CO_3 in acetone (R. T.), followed by pyridine/SMe_2 ligand exchange at room temperature.

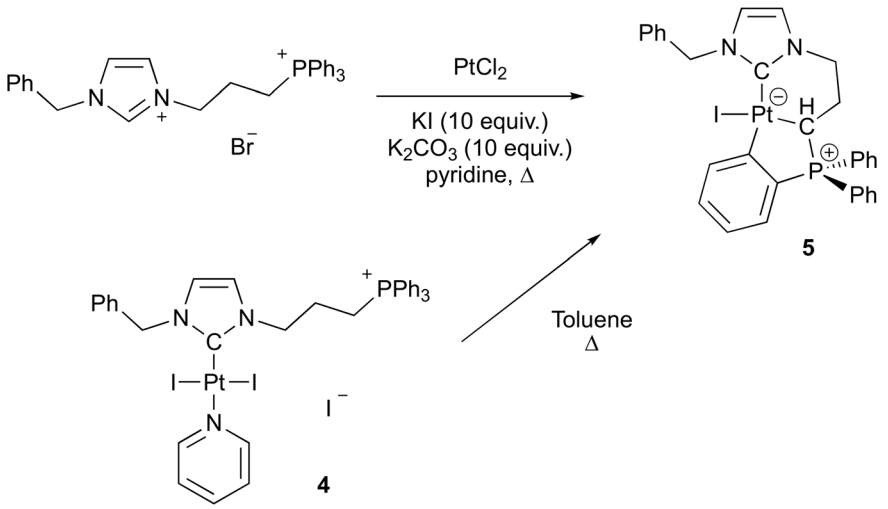

Fig. 2 Observed double C–H activation upon heating the triphenylphosphonium-functionalized Pt NHC complex **4** or direct synthesis of **5** starting from the corresponding imidazolium precursor.

conventional organic solvents. In the context of biological experiments, the dissolution of the compound in dimethyl sulfoxide (DMSO) can be followed by dilution in an aqueous medium, which will serve as the study reference. It is important to note that previous NMR studies have shown that these complexes are perfectly stable in DMSO solution at 37 °C.

While active molecules can be formulated in liposomes at room temperature, the situation is different when it comes to generating lipid nanocapsules, which requires temperature close to 100 °C (*vide infra*). Therefore, the three molecules were exposed in toluene-d^8 solution at 100 °C overnight to study their stability under these conditions. While the first two remained unchanged, the *in situ* study showed that complex **3** is not stable and decomposes. Changing the adamantyl group of complex **3** to phenyl provided a clearer picture, since the product resulting from heating could be easily crystallized and fully characterized (Fig. 2). In particular, X-ray diffraction analyses enabled the molecular structure of the complex to be determined unambiguously. Complex **5** is the result of two C–H bond activations, featuring a C-coordinated phosphonium ylide and a C-aromatic bond. Alternatively, the zwitterionic Pt complex **5** could be synthesized directly from the ligand precursor using a classical procedure starting from platinum chloride.

Fig. 3 displays the molecular structure of compound **5**. The platinum atom is situated in a slightly distorted square-planar environment, because of a constrained arrangement of the ligand composed of a five-membered and a six-membered metallacycle. The bond lengths of C_{NHC}–Pt, C_{ylide}–Pt and C_{Ph}–Pt are respectively 2.049(3) Å, 2.091(3) Å and 2.067(3) Å and the NHC is situated in a *trans* position to the phenyl fragment with an angle [C(1)–Pt(1)–C(22)] of 171.95(13)°. The iodide and the CH from the ylide are arranged *trans* to each other with [C(19)–Pt(1)–I(1)] of 170.22°. This type of molecular arrangement has recently been observed with ligands of the same type in the case of palladium.[62]

Prior to encapsulation, the lipophilicity of the molecules has been quantified, which may impact not only solubility and toxicity but also various other factors such as absorption, distribution, metabolization and excretion.[63] All three compounds presented log*P* values of approximately 1 (*i.e.* 1.05 ± 0.18, 0.91 ± 0.25 and 0.94 ± 0.12, respectively for **1**, **2** and **3**) confirming that they are indeed lipophilic compounds compared to cisplatin (−2.21) and oxaliplatin (−1.39)[64,65] which are, in contrast, hydrophilic. Compared to **1** and **2**, we can note that the introduction of the triphenylphosphonium group does not change the lipophilicity of compound **3**.

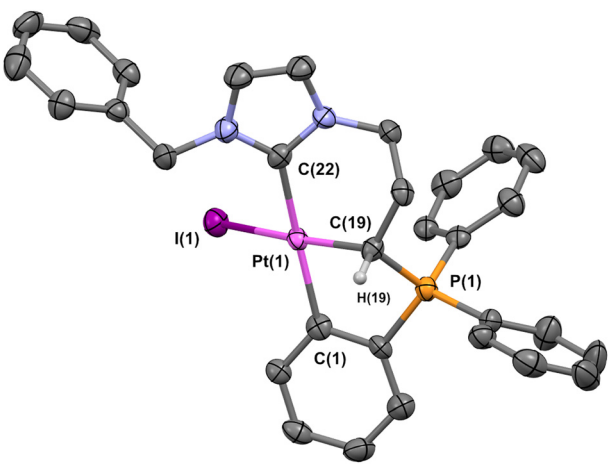

Fig. 3 ORTEP view of *ortho*-metalated complex **5**. Thermal ellipsoids set at the 60% probability level, hydrogen atoms are omitted, except for the ylide function. Selected distances (Å) and angles (°): C(22)–Pt(1), 2.049(3); C(1)–Pt(1), 2.067(3); Pt(1)–I(1), 2.688(3); C(19)–Pt(1), 2.091(3); P(1)–C(19), 1.788(3); C(22)–Pt(1)–I(1), 94.82(9), C(22)–Pt(1)–C(19), 88.17(13); C(1)–Pt(1)–I(1), 92.24(9); C(1)–Pt(1)–C(19), 85.49(13); C(22)–Pt(1)–C(1), 171.95(13); I(1)–Pt(1)–C(19), 170.22(9). CCDC-2373163.

Encapsulation into liposomes

The NHC platinum complexes were formulated by thin lipid hydration followed by sonication (*i.e.* Bangham method).[66] The liposomes were constituted by phosphatidylcholine (PC, a zwitterionic lipid), phosphatidylglycerol (PG, a negatively charged lipid) and cholesterol (neutral) resulting in a negative zeta potential of −35.6 mV ± 3.2 (for empty liposomes). Then, all three complexes were encapsulated at a final concentration of 0.5 mM. With regard to the stability of formulations containing NHC-Pt complexes, the diameter and polydispersity index (PDI) were evaluated by dynamic light scattering (DLS) after the formulation process, before freezing and after thawing. The results are shown in Table 1. The nanoparticle diameters for all complexes were below 100 nm and PDIs were below 0.300, indicating that the samples were monodisperse. After freezing in the presence of D-glucose as a cryoprotectant, the sizes remained <100 nm with PDIs not greater than 0.300 regardless of the encapsulated complex. The empty liposomes also exhibited no alteration in parameter values in comparison with the liposomes loaded with **1** or **3**, indicating that the thawing process did not induce any changes. The liposome loaded with **2**, on the other hand, sees its particle size reduced by almost a factor two. As the latter formulation has shown limited stability over time, we did not study it further.

Having established the reproducibility and stability of liposomes loaded with **1** and **3**, we carried out assays to quantify the platinum. The encapsulation efficiency and the drug loading were evaluated by inductively coupled plasma mass spectroscopy (ICP-MS). An encapsulation efficiency of 22% was achieved with neutral Pt complex **1**, whereas an efficiency of nearly 100% was observed with the cationic Pt complex **3** (Table 1). The drug loadings within the liposomes compared to all other components are therefore 0.46 ± 0.04% and 4.5 ± 0.1%, respectively.

Based on these results, we then set about preparing neutral or positively-charged liposomes. Neutral liposomes were obtained from phosphatidylcholine (PC) and cholesterol and positively charged liposomes included 1,2-dioleoxy-3(trimethylammonium) propane chloride (DOTAP). While the characterization of these formulations confirmed the nanometric size of the empty or loaded Pt NHC liposomes (*i.e.*, 50–70 nm), the stability of these formulations was not sufficient to continue the study. In particular, after freezing and thawing, the key parameters were not retained with both types of liposomes (Table S1†).

Encapsulation into lipid nanocapsules

The second delivery system that was tested consisted of lipid nanocapsules (LNCs).[67] The LNCs were formulated using triglycerides, lecithin and polyethylene glycol hydroxystearate[68] and NHC-Pt complexes **1** and **2** were encapsulated at a concentration of 1 mM. Preliminary studies of the stability of **3** had shown a possible deactivation process, so we carried out a series of experiments consisting of subjecting a solution of **3** in DMSO to one heating cycle at 100 °C, out of the three cycles required for the LNC formulation process, lasting around one minute. After this experiment, the heated complex and unheated complex were tested *in vitro* (NCH421K cells) and it was observed that the heating of the complex resulted in a loss of cytotoxicity of approximately three times at a concentration of 0.5 μM (see ESI,† Fig. S2). Complex **3** was therefore not studied when encapsulated in LNCs.

Table 2 displays the physicochemical characterization of LNCs. The diameter of the LNC formulations was found to be 59 nm and 53 nm when loaded with complexes **1** and **2**, respectively. These systems presented very low PDIs, below 0.100, indicating a high degree of monodispersity within the samples. The encapsulation efficiency evaluated by inductively coupled plasma mass spectroscopy (ICP-MS) was nearly 100% for both nano systems. The drug loadings were found to be 0.36% and 0.22%, respectively. Reproducibility of liposome and nanocapsule formulations in terms of diameter was also confirmed in both cases (see ESI,† Fig. S1).

Cytotoxicity assessment of liposomal and nanocapsule-formulated NHC-Pt complexes

The reproducibility of the encapsulation having been demonstrated, we evaluated the cytotoxicity of free and encapsulated molecules on several types of cancer cells including glioblastoma cells (U87) and cancer stem cells (NCH421K). To do this, we cultivated them for 24 hours and tested mitochondrial activity, which is proportional to cell viability, using the CellTiter Glo® 3D test. The IC_{50} were determined for the unformulated NHC-Pt complexes **1–3** and formulated in liposomes and/or in lipid nanocapsules after 24 h of treatment. The three NHC-Pt complexes were first tested

Table 1 Diameter and PDI of empty and loaded liposomes by complexes **1–3**. They were measured immediately after their formulation before freezing and post-thawing by DLS (intensity values for diameter). The post-thawing values were recorded before the start of each *in vitro* experiment and the mean is shown (PDI: polydispersity index)

	Before freezing		Post-thawing			
Content	Diameter (nm)	PDI	Diameter (nm)	PDI	Encapsulation efficiency (%)	Drug loading (%)
1	82 ± 9	0.245	78 ± 9	0.232	22	0.46 ± 0.04
2	82 ± 9	0.245	44 ± 7	0.300	—	—
3	59 ± 10	0.219	59 ± 8	0.219	100	4.5 ± 0.1
None	93 ± 11	0.179	84 ± 10	0.196	—	—

Table 2 Physicochemical characterization of the LNCs loaded with complexes **1** or **2**, measured by DLS. Encapsulation efficiency and drug loading values were determined using ICP-MS

Content	Diameter (nm)	PDI	Encapsulation efficiency (%)	Drug loading (%)
1	59 ± 6	0.037	98.0 ± 12.0	0.22 ± 0.03
2	53 ± 5	0.070	99.2 ± 2.0	0.36 ± 0.01
None	57 ± 4	0.070	—	—

on the glioblastoma stem cells (NCH421K),[69] the more differentiated glioma cell line U87-MG TMZ sens. (which is sensitive to temozolomide) and the colon cancer cell line (HCT116) serving as a cancer cell line reference with our previous studies.[39] Commercial oxaliplatin dissolved in water was used as a control. Table 3 shows the IC_{50} values for each system which were normalized with respect to the blank vectors as well as to the encapsulation efficiency of each system.

The results show that both the free and the encapsulated NHC-Pt complexes are significantly more cytotoxic after 24 h of treatment than oxaliplatin against all of these cell lines. Importantly, there is no significant difference between the IC_{50} of the free compounds and that of their encapsulated counterparts for each cell line, validating *in vitro* the formulation strategy for this type of compound. It is important to mention that the determination of certain values was not possible for complexes **1** and **2**. This was due to the high level of toxicity exhibited by the blank systems (a phenomenon that is likely attributable to the low drug loading values). In these cases, only a minimum value could be determined (see Table 3).

On cancer stem cells NCH421K, complexes **1** and **3** showed very good cytotoxic activities ($0.2 < IC_{50} < 0.9$ μM) whatever the formulation, whereas oxaliplatin was poorly active (IC_{50} = 158 μM). On U87-MG TMZ sensitive cancer cells, the best result was obtained with complex **3** formulated in liposomes with an IC_{50} of 1.2 μM. The two complexes also displayed good activities on HCT116 cancer cells ($IC_{50} < 2$ μM). In contrast, the nitro-functionalized Pt complex **2** performed less well than the two other compounds on the three cell lines which were tested – although it has to be noted that **2** was still more active than oxaliplatin.

Altogether, we found that complex **3** encapsulated in negatively charged liposomes was the best combination, showing high encapsulation efficiency and very good (and unaltered compared to the free drug) cytotoxicity against the three cell lines tested. The study was therefore continued on three other differentiated glioblastoma cancer cell lines, namely U87-MG, U251-MG, and GL261, all of which have stereotaxic mouse models.[70–74] Against these three cell lines, the results show that the cytotoxicity of the complex encapsulated into liposomes was preserved.

Cellular uptake on HCT116

Following these results, the cellular uptake of the liposomal complex **3** by colon cancer HCT116 cells was studied and compared to its free counterpart and oxaliplatin by analyzing the Pt inside the cells using ICP-MS. This was done to determine if the encapsulation of the complexes enhanced Pt accumulation within the cells.

The experiment was carried out using the same concentration for all tested compounds for comparative purposes, 5 μM, which was deemed sufficient for platinum detection by ICP-MS. Two incubation times were tested, 4 h and 6 h at 37 °C, which were short to minimize cytotoxicity on the cells to focus on the uptake of complexes. Following incubation, cells were harvested, washed, lysed, and the intracellular and extracellular Pt contents were quantified by ICP-MS. The data revealed that there was no difference between 4 h and 6 h (same order of magnitude). However, it should be mentioned that this could be attributed to the onset of cell death at 6 h resulting in the release of platinum into the medium. Examination of the data after 4 hours of incubation (Fig. 4) shows identical results for the uptake of the liposome-encapsulated complex and its non-encapsulated counterpart (*ca.* 5% of Pt detected) and 0.25% was detected in the cells for oxaliplatin.

Table 3 *In vitro* cytotoxicity investigations. IC_{50} values (μM) of the NHC-Pt complexes as a function of the formulation: water/DMSO, liposomes or lipid nanocapsules (LNCs) after 24 h at 37 °C of treatment on glioblastoma cancer stem cells (NCH421K), glioblastoma differentiated cancer cells (U87-MG TMZ sensitive, U87-MG, U251-MG and GL261) and colon cancer cells (HCT116). IC_{50} values were determined by at least three independent assays ± one standard error of the mean (SEM). Each experiment was carried out in at least a technical triplicate. IC_{50} values were calculated by non-linear regression of cell viability curves generated *via* CellTiter Glo® 3D cell viability assay using Prism software. Statistics represent one-way ANOVA test. U87-MG TMZ sens: $p < 0.01$, NCH421K or HCT166: $p < 0.0001$ comparing all the compounds with oxaliplatin for that specific cell line. ND = non-determined values

Complex	Formulation	NCH421K	U87-MG TMZ sens.	HCT116	U87-MG	U251-MG	GL261
1	H_2O/DMSO	0.3 ± 0.03	2.8 ± 0.4	1.6 ± 0.3	ND		
	Liposome	0.2 ± 0.04	>4.3[a]	2.0 ± 0.9			
	LNC	0.9 ± 0.2	>2.5[a]	>10[a]			
2	H_2O/DMSO	4.5 ± 0.6	21.6 ± 3.7	14.5 ± 3.5			
	LNC	5.8 ± 1.2	>2.5[a]	8.4 ± 0.4			
3	H_2O/DMSO	0.5 ± 0.2	2.0 ± 0.1	1.7 ± 0.5	1.8 ± 0.5	1.9 ± 1.1	0.8 ± 0.3
	Liposome	0.3 ± 0.2	1.2 ± 0.2	1.4 ± 0.3	1.9 ± 1.0	2.7 ± 1.1	0.7 ± 0.5
Oxaliplatin	H_2O	158 ± 20	164 ± 55	79 ± 21	ND		

[a] Values for which the IC_{50} couldn't be evaluated due to the cytotoxicity of the nanovector alone.

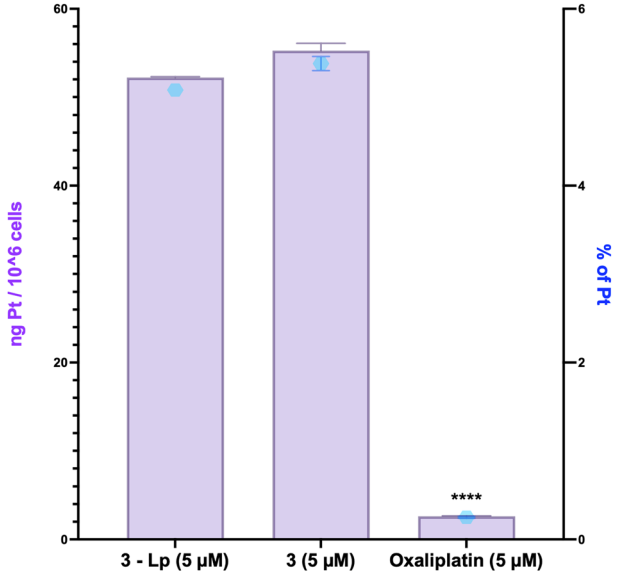

Fig. 4 Comparison of the cellular uptake of free complex **3** and encapsulated in liposomes **3** – **LP** in HCT116 cells after 4 h of incubation with 5 μM of Pt for each sample at 37 °C and quantified by ICP-MS. Oxaliplatin was used as a reference. The cellular uptake is expressed in ng $Pt/10^6$ cells by purple bars (left *Y* axis) and in percentage of platinum content by blue dots (right *Y* axis) detected within cells. The graph was generated using GraphPad Prism 8 software. *N* = 3. The statistical analysis was done by performing an ordinary one-way ANOVA test between each group and the control group (oxaliplatin) (**** = $p < 0.0001$).

These results demonstrate that liposomal encapsulation of complex **3** does not significantly enhance its cellular uptake in HCT116 colon cancer cells compared to its free form, with both showing similar levels of intracellular platinum accumulation after 4 hours of incubation. In contrast, oxaliplatin showed much lower uptake under the same conditions. Altogether, these findings support the suitability of the liposomal formulation for delivering complex **3** without altering its ability to reach intracellular targets, while still offering the advantages of a nano-delivery system, such as dissolving the complex in an aqueous media.

In vivo evaluation of complex 3 encapsulated in liposomes on a U87-MG glioblastoma mouse model

To go one step further, complex **3** – free and formulated in liposomes – was tested *in vivo* on 6-week-old NMRI nude female mice using the U87-MG glioblastoma model. Before starting the study, a toxicity assay was undertaken to evaluate which concentration of the complex could be injected into the mice without having secondary effects (see ESI,† Fig. S3 and S4). A concentration of 0.6 mg kg^{-1} was selected for the *in vivo* study as it didn't demonstrate any adverse effect on the mice.

In the *in vivo* assay four different mouse groups were considered: mice treated with the vehicle solution of NaCl 0.9%, mice treated with 0.2 mg kg^{-1} of oxaliplatin (equivalent amount of platinum to that of the injected complex **3**), mice treated with 0.6 mg kg^{-1} of **3** encapsulated within liposomes, and mice treated with 0.6 mg kg^{-1} of **3** solubilized in water/DMSO. Treatments began with intra-tumoral injections on day 27 after implantation of differentiated U87-MG glioblastoma cells (Fig. 5). At this step, the mice were sorted into four groups randomly with similar initial mean tumor volumes (see ESI,† Fig. S6). After three sessions of intratumoral treatment, all three treatments began to show an inhibitory effect on tumor growth compared with the NaCl control group. Thereafter, tumor volume increased significantly in all groups. However, a difference between oxaliplatin and complex **3** is rapidly observed. From day 34 onward, tumor size differences become progressively significant. Mice treated with oxaliplatin exhibit notably smaller tumors compared to the NaCl control group (p-value < 0.0001), although tumors remain significantly larger than those treated with DMSO-**3** (p-value = 0.0425). Similarly, treatment with Lp-**3** results in a significant tumor size reduction compared to the NaCl group (p-value < 0.0001). Importantly, mice receiving the encapsulated complex Lp-**3** show tumor sizes comparable to those treated with **3** in DMSO (p-value = 0.0425).

No toxicity was revealed by the monitoring of the body weight after implantation of the U87-MG glioblastoma differentiated cells (see ESI,† Fig. S7). However, from day 38, some mice were killed due to their tumor volume which reached ethical limits. The end of the experiment was analyzed in the form of a survival study (Fig. 6). This shows that mice treated with the liposome-encapsulated complex **3**

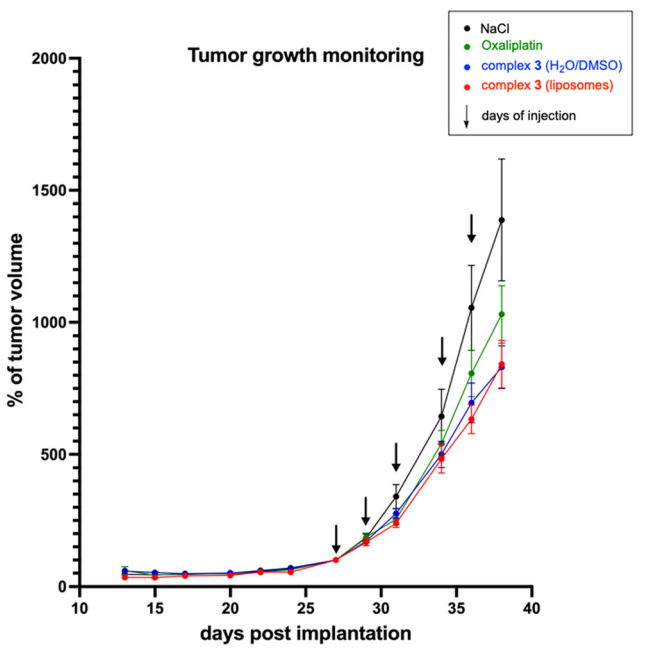

Fig. 5 Tumor growth (%) kinetic *in vivo* results over time (in days post-implantation of the tumors). The intra-tumoral injections are indicated with an arrow. The graph was generated using GraphPad Prism 8 software (statistical data in the ESI†).

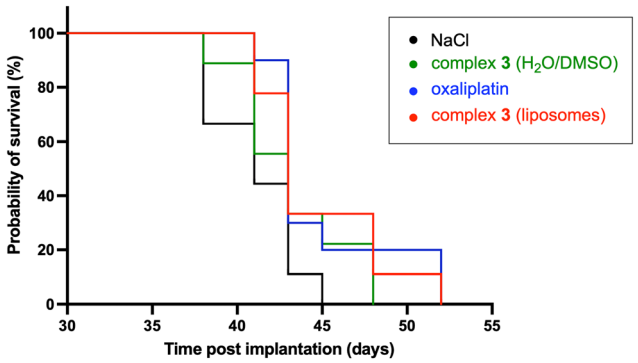

Fig. 6 Survival curves. The graph was generated using GraphPad Prism 8 software (see ESI,† Fig. S8 for statistical data).

and those treated with oxaliplatin survived a maximum of 52 days after tumor implantation, compared with those treated with the complex **3** in solution, which survived a maximum of 48 days. Control mice survived for only 45 days. These results suggest that the liposomal formulation of **3** is at least as effective *in vivo* – if not more – in increasing overall survival in mice and in its anti-tumor effect than the free drug solubilized in DMSO/water.

Discussion

For more than a decade, NHC carbene ligands have profoundly influenced the domain of inorganic medicinal chemistry.[42] The stability of the metal–ligand bond in these systems means that molecular integrity is preserved and the complex does not decompose too rapidly *in vivo*, which is one of the problems observed with conventional platinum compounds such as cisplatin. Numerous studies have shown these compounds to have higher cytotoxicity than cisplatin, with encouraging *in vivo* results.[40] Furthermore, the mechanisms of action of these compounds, which incorporate several pathways, have been shown to overcome the chemoresistance that has been observed with conventional Pt compounds. In addition, the mitochondrial alteration induced by some NHC metal complexes offers the possibility of inducing cell death mechanisms that overcome the chemoresistance associated with the cell nucleus.[40,43,45] The interest in targeting the mitochondria also lies in the possibility of eradicating CSCs, which play an important role in the therapeutic resistance of several cancers. Cancer stem cells (CSCs) could explain many of the shortcomings of existing chemotherapy treatments.[75,76]

Here, we wanted to take the development of these systems a step further by addressing the solubilization challenge of mitochondria-targeting NHC-Pt complexes in water to avoid the use of DMSO and other organic solvents. Three NHC platinum candidates were selected for formulation either as liposomes or lipid nanocapsules, namely complexes **1**, **2** and **3** (Fig. 1). In particular, we have recently demonstrated that compound **3** with the mitochondria-targeting triphenylphosphonium moiety produces significant reactive oxygen species in mitochondria.[45]

Unlike cisplatin, these compounds are lipophilic, as shown by log*P* measurements. The encapsulation of the three complexes was investigated by encapsulation in positive, neutral or negatively-charged liposomes. The stability of these objects being essential for potential applications, we subjected them to a freezing in the presence of a cryoprotectant and thawing cycle (Table 1 and Table S1†). While the results obtained with the neutral and positive liposomes were disappointing (Table S1†), the negatively charged liposomes with complexes **1** and **3** proved to be unaffected after a freeze/thaw cycle. On the other hand, results with the nitro-functionalized complex **2** were not satisfactory in terms of stability (Table 1, entry 2). The absence of the adamantyl substituent in complex **2** is likely a key contributing factor, which may influence the overall packing and structural organization within the liposomal bilayer. Finally, platinum ICP-MS analyses revealed that the encapsulation efficiency with **3** was quantitative, a result to be compared with only 22% for the neutral compound **1**. Thus, the cationic nature of the platinum triphenylphosphonium complex, combined with a negatively charged liposome, favors the quantitative formulation of the active ingredient.

Other delivery systems using lipid nanocapsules have been investigated for the formation of these NHC platinum complexes. Neutral Pt compounds **1** and **2** were readily encapsulated in well-defined objects with an average size of 50–60 nm, albeit with a relatively low platinum loading of 0.2–0.4 wt% (Table 2). Attempts to encapsulate platinum derivative **3** have proved unsuccessful, and the study of the molecule's stability seems to be a determining factor in this respect. It has been demonstrated that exposure of the parent complex **4** to a temperature of merely 100 °C instigates a reaction involving a double C–H activation, thus yielding as an identified product the Pt zwitterionic species **5** (Fig. 2). The molecular structure was confirmed by X-ray diffraction studies as displayed in Fig. 3.

The biological activity of all these systems was studied *in vitro* for the unformulated NHC-Pt complexes **1**–**3** and formulated in liposomes and/or in lipid nanocapsules (Table 3). Whatever the formulation, compounds **1** and **3** were found to be highly active on cancer stem cells NCH421K, in contrast to oxaliplatin which was poorly active. The same conclusion can be drawn on cancer cells U87-MG TMZ sensitive and HCT116. However, the result with the nitro compound **2** did not give the expected results. Of the two formulations studied, the liposome formulation was more effective for *in vitro* activities, particularly with compound **3**, which is characterized by a much higher level of active ingredient. The conclusive results with **3** have been confirmed with other cells such as U87-MG, U251-MG and GL261 cell lines (Table 3, right). Finally, cellular uptake investigation of the nano-encapsulated complex **3** compared to its free counterpart and oxaliplatin revealed no discernible difference between the uptake of the liposome-encapsulated complex and its non-encapsulated counterpart, with approximately 5% platinum detected in the cells (*vs.* 0.25% for oxaliplatin).

The results of this study provide robust evidence that complex **3** in liposomes is a promising formulation, opening up new research prospects such as *in vivo* studies. Consequently, an experiment was conducted on NMRI nude female mice using the U87-MG glioblastoma model. Intratumoral injections were employed as a first proof-of-concept as the primary aim was to evaluate the targeting capability and cytotoxic efficacy of the formulated Pt complex in a controlled tumor environment. Fig. 5 displays the evolution of the volume of the tumors as a function of days and type of treatment (*i.e.*, NaCl control, oxaliplatin, complex **3** in water/DMSO and complex **3** in liposomes). The oxaliplatin-treated mice had significantly smaller tumors compared with the control group, and larger tumors compared with mice treated with **3**. The results also demonstrate that the formulation of the NHC complex in liposomes does not affect its activity, since the results are identical to those obtained with a direct formulation in water/DMSO solution. Survival curves from *in vivo* studies are consistent with these results revealing that treatment with oxaliplatin or complex **3** in liposomes results in 7-day increased survival of mice bearing aggressive glioblastoma compared to untreated mice and 4-day increased survival compared to mice treated with complex **3** dissolved in the presence of DMSO. All these results suggest that **3** formulated in liposomes could compare favorably with oxaliplatin for tumor treatment. Furthermore, in the future, functionalization of the liposome with ligands could be an interesting tool for the establishment of active targeting of the vector towards target tumor cells.

Conclusion

In conclusion, the encapsulation of cytotoxic platinum *N*-heterocyclic carbene complexes has been investigated using either liposomes or lipid nanocapsules. It is important to note that both of these possibilities are viable alternatives for avoiding the use of organic solvents, which is still the method used for these types of complexes, which are insoluble in water. Liposomal formulations have proved to be the most promising in terms of both stability and efficacy. It is noteworthy that the cytotoxic activity was retained on both cancer cells and cancer stem cells, particularly for the NHC platinum complex **3** functionalized by the mitochondria-targeting agent. Moreover, *in vivo* tests with Pt complex **3** (encapsulated or not) demonstrated superior outcomes in comparison to the conventional oxaliplatin Pt complex. These findings highlight the need to focus on optimizing the formulation of NHC carbene-based anticancer drugs, aiming to reduce toxicity and enhance therapeutic efficacy. This priority becomes especially important given the growing number of organometallic complexes studied under experimental conditions that do not readily support clinical translation.

Data availability

The data supporting this article have been included as part of the ESI.†

Crystallographic data of complex **5** have been deposited at the Cambridge Crystallographic Data Centre (CCDC) 2373163.

Conflicts of interest

There is no conflict of interest to declare.

Acknowledgements

This work was supported by the Interdisciplinary Institute HiFunMat, as part of the ITI 2021-2028 program of the University of Strasbourg, CNRS and Inserm *via* the IdEx Unistra (ANR-10-IDEX-0002) and SFRI-STRAT'US (ANR-20-SFRI-0012) under the framework of the French Investments for the Future Program. This work was also financially supported by the Fondation ARC project Number ARCPJA32020060002306 (S. F.), La Ligue contre le Cancer CCIR Est (2023) and Carnot MICA (2024 GLIOBLAT). We would like to extend our gratitude to Dr. Anne Boos, Islah El Masoudi and Pascale Ronot (Plateforme Analytique des Inorganiques, ECPM) for their valuable contributions to the platinum dosage by ICP-MS and to Marie-Noëlle Lalloz-Vogel for her contribution to the synthesis of chemicals. We would also like to sincerely thank Dr. Emmanuel Garcion, from the Inserm U1232 CRCINA équipe 17 in Angers, for providing the U87-MG, GL261 and U251-MG cell lines. Additionally, we would like to show our deep appreciation to Dr. Julien Vollaire and Dr. Véronique Josserand working at the Plateforme OPTIMAL – Imagerie optique du petit Animal at the Institute for Advanced Biosciences (Grenoble, France) for their participation in conducting the *in vivo* studies.

References

1 H. Strobel, T. Baisch, R. Fitzel, K. Schilberg, M. D. Siegelin, G. Karpel-Massler, K. M. Debatin and M. A. Westhoff, *Biomedicines*, 2019, **7**, 69.
2 S. Mukherjee and P. P. Pillai, *Biochim. Biophys. Acta, Gen. Subj.*, 2022, **1866**, 130065.
3 L. Shabani, M. Abbasi, M. Amini, A. M. Amani and A. Vaez, *J. Neurol. Sci.*, 2022, **440**, 120316.
4 N. Iturrioz-Rodriguez, N. Sampron and A. Matheu, *Theranostics*, 2023, **13**, 2734–2756.
5 T. Reya, S. J. Morrison, M. F. Clarke and I. L. Weissman, *Nature*, 2001, **414**, 105–111.
6 S. K. Singh, C. Hawkins, I. D. Clarke, J. A. Squire, J. Bayani, T. Hide, R. M. Henkelman, M. D. Cusimano and P. B. Dirks, *Nature*, 2004, **432**, 396–401.
7 A. R. Safa, M. R. Saadatzadeh, A. A. Cohen-Gadol, K. E. Pollok and K. Bijangi-Vishehsaraei, *Genes Dis.*, 2015, **2**, 152–163.
8 M. Venere, H. A. Fine, P. B. Dirks and J. N. Rich, *Glia*, 2011, **59**, 1148–1154.
9 C. McCartin, E. Mathieu, M. Dontenwill, C. Herold-Mende, A. Idbaih, A. Bonfiglio, M. Mauro, S. Fournel and A. Kichler, *Chem.-Biol. Interact.*, 2022, **367**, 110167.

10 C. Rancoule, J. B. Guy, A. Vallard, M. Ben Mrad, A. Rehailia and N. Magne, *Bull. Cancer*, 2017, **104**, 167–176.
11 E. Martinez-Balibrea, A. Martinez-Cardus, A. Gines, V. Ruiz de Porras, C. Moutinho, L. Layos, J. L. Manzano, C. Buges, S. Bystrup, M. Esteller and A. Abad, *Mol. Cancer Ther.*, 2015, **14**, 1767–1776.
12 B. Rosenberg, L. Vancamp and T. Krigas, *Nature*, 1965, **205**, 698–699.
13 D. Wisher, *J. Med. Libr. Assoc.*, 2012, **100**, 75–76, DOI: **10.3163/1536-5050.3100.3161.3018**.
14 S. Dasari and P. B. Tchounwou, *Eur. J. Pharmacol.*, 2014, **740**, 364–378.
15 J. E. Perez, S. Fritzell, J. Kopecky, E. Visse, A. Darabi and P. Siesjo, *Sci. Rep.*, 2019, **9**, 5632.
16 J. Jeon, S. Lee, H. Kim, H. Kang, H. Youn, S. Jo, B. Youn and H. Y. Kim, *Int. J. Mol. Sci.*, 2021, **22**, 5111.
17 N. B. Roberts, A. S. Wadajkar, J. A. Winkles, E. Davila, A. J. Kim and G. F. Woodworth, *Onco Targets Ther*, 2016, **5**, e1208876.
18 A. Arshad, B. Yang, A. S. Bienemann, N. U. Barua, M. J. Wyatt, M. Woolley, D. E. Johnson, K. J. Edler and S. S. Gill, *PLoS One*, 2015, **10**, e0132266.
19 Y. Miura, T. Takenaka, K. Toh, S. Wu, H. Nishihara, M. R. Kano, Y. Ino, T. Nomoto, Y. Matsumoto, H. Koyama, H. Cabral, N. Nishiyama and K. Kataoka, *ACS Nano*, 2013, **7**, 8583–8592.
20 B. Ferrari, E. Roda, E. C. Priori, F. De Luca, A. Facoetti, M. Ravera, F. Brandalise, C. A. Locatelli, P. Rossi and M. G. Bottone, *Front. Neurosci.*, 2021, **15**, 589906.
21 D. Bourissou, O. Guerret, F. P. Gabbaï and G. Bertrand, *Chem. Rev.*, 2000, **100**, 39–92.
22 W. A. Herrmann, *Angew. Chem., Int. Ed.*, 2002, **41**, 1290–1309.
23 V. Cesar, S. Bellemin-Laponnaz and L. H. Gade, *Chem. Soc. Rev.*, 2004, **33**, 619–636.
24 L. Mercs and M. Albrecht, *Chem. Soc. Rev.*, 2010, **39**, 1903–1912.
25 L. Benhamou, E. Chardon, G. Lavigne, S. Bellemin-Laponnaz and V. César, *Chem. Rev.*, 2011, **111**, 2705–2733.
26 S. Bellemin-Laponnaz and S. Dagorne, *Chem. Rev.*, 2014, **114**, 8747–8774.
27 M. L. Teyssot, A. S. Jarrousse, M. Manin, A. Chevry, S. Roche, F. Norre, C. Beaudoin, L. Morel, D. Boyer, R. Mahiou and A. Gautier, *Dalton Trans.*, 2009, 6894–6902, DOI: **10.1039/b906308k**.
28 M. Monticelli, S. Bellemin-Laponnaz, C. Tubaro and M. Rancan, *Eur. J. Inorg. Chem.*, 2017, **2017**, 2488–2495.
29 M. Baron, S. Bellemin-Laponnaz, C. Tubaro, M. Basato, S. Bogialli and A. Dolmella, *J. Inorg. Biochem.*, 2014, **141**, 94–102.
30 M. Malik, D. C. Bienko, U. K. Komarnicka, A. Kyziol, M. Drys, A. Switlicka, E. Dyguda-Kazimierowicz and W. Jedwabny, *J. Inorg. Biochem.*, 2021, **215**, 111311.
31 G. Gasser, I. Ott and N. Metzler-Nolte, *J. Med. Chem.*, 2011, **54**, 3–25.
32 A. Gautier and F. Cisnetti, *Metallomics*, 2012, **4**, 23–32.
33 C. G. Hartinger, N. Metzler-Nolte and P. J. Dyson, *Organometallics*, 2012, **31**, 5677–5685.
34 W. Liu and R. Gust, *Coord. Chem. Rev.*, 2016, **329**, 191–213.
35 T. Zou, C. N. Lok, P. K. Wan, Z. F. Zhang, S. K. Fung and C. M. Che, *Curr. Opin. Chem. Biol.*, 2018, **43**, 30–36.
36 M. Porchia, M. Pellei, M. Marinelli, F. Tisato, F. Del Bello and C. Santini, *Eur. J. Med. Chem.*, 2018, **146**, 709–746.
37 M. Mora, M. C. Gimeno and R. Visbal, *Chem. Soc. Rev.*, 2019, **48**, 447–462.
38 S. Y. Hussaini, R. A. Haque and M. R. Razali, *J. Organomet. Chem.*, 2019, **882**, 96–111.
39 S. Bellemin-Laponnaz, *Eur. J. Inorg. Chem.*, 2020, **2020**, 10–20.
40 N. Chekkat, G. Dahm, E. Chardon, M. Wantz, J. Sitz, M. Decossas, O. Lambert, B. Frisch, R. Rubbiani, G. Gasser, G. Guichard, S. Fournel and S. Bellemin-Laponnaz, *Bioconjugate Chem.*, 2016, **27**, 1942–1948.
41 M. Chtchigrovsky, L. Eloy, H. Jullien, L. Saker, E. Segal-Bendirdjian, J. Poupon, S. Bombard, T. Cresteil, P. Retailleau and A. Marinetti, *J. Med. Chem.*, 2013, **56**, 2074–2086.
42 M. Skander, P. Retailleau, B. Bourrie, L. Schio, P. Mailliet and A. Marinetti, *J. Med. Chem.*, 2010, **53**, 2146–2154.
43 C. McCartin, C. Dussouillez, C. Bernhard, E. Mathieu, J. Blumberger, M. Dontenwill, C. Herold-Mende, A. Idbaih, P. Lavalle, S. Bellemin-Laponnaz, A. Kichler and S. Fournel, *Cancers*, 2022, **14**, 5057.
44 C. McCartin, J. Blumberger, C. Dussouillez, P. Fernandez de Larrinoa, M. Dontenwill, C. Herold-Mende, P. Lavalle, B. Heurtault, S. Bellemin-Laponnaz, S. Fournel and A. Kichler, *J. Funct. Biomater.*, 2022, **14**, 17.
45 P. Fernandez de Larrinoa, J. Parmentier, A. Kichler, T. Achard, M. Dontenwill, C. Herold-Mende, S. Fournel, B. Frisch, B. Heurtault and S. Bellemin-Laponnaz, *Int. J. Pharm.*, 2023, **641**, 123071.
46 E. Vlashi, C. Lagadec, L. Vergnes, T. Matsutani, K. Masui, M. Poulou, R. Popescu, L. Della Donna, P. Evers, C. Dekmezian, K. Reue, H. Christofk, P. S. Mischel and F. Pajonk, *Proc. Natl. Acad. Sci. U. S. A.*, 2011, **108**, 16062–16067.
47 G. Farnie, F. Sotgia and M. P. Lisanti, *Onco Targets Ther*, 2015, **6**, 30472–30486.
48 M. G. Lampugnani, M. Pedenovi, A. Niewiarowski, B. Casali, M. B. Donati, G. C. Corbascio and P. C. Marchisio, *Exp. Cell Res.*, 1987, **172**, 385–396.
49 A. F. Davidson, C. Glasscock, D. R. McClanahan, J. D. Benson and A. Z. Higgins, *PLoS One*, 2015, **10**, e0142828.
50 M. Awan, I. Buriak, R. Fleck, B. Fuller, A. Goltsev, J. Kerby, M. Lowdell, P. Mericka, A. Petrenko, Y. Petrenko, O. Rogulska, A. Stolzing and G. N. Stacey, *Regener. Med.*, 2020, **15**, 1463–1491.
51 C. Yuan, J. Gao, J. Guo, L. Bai, C. Marshall, Z. Cai, L. Wang and M. Xiao, *PLoS One*, 2014, **9**, e107447.
52 W. J. Youngs, A. R. Knapp, P. O. Wagers and C. A. Tessier, *Dalton Trans.*, 2012, **41**, 327–336.
53 L. Ronga, M. Varcamonti and D. Tesauro, *Molecules*, 2023, **28**, 4435.

54 H. A. Mohamed, M. Khuphe, S. J. Boardman, S. Shepherd, R. M. Phillips, P. D. Thornton and C. E. Willans, *RSC Adv.*, 2018, **8**, 10474–10477.
55 Y. Marciano, V. Del Solar, N. Nayeem, D. Dave, J. Son, M. Contel and R. V. Ulijn, *J. Am. Chem. Soc.*, 2023, **145**, 234–246.
56 R. D. Hofheinz, S. U. Gnad-Vogt, U. Beyer and A. Hochhaus, *Anti-Cancer Drugs*, 2005, **16**, 691–707.
57 H. Cabral and K. Kataoka, *J. Controlled Release*, 2014, **190**, 465–476.
58 G. Dahm, M. Bouché, C. Bailly, L. Karmazin and S. Bellemin-Laponnaz, *J. Organomet. Chem.*, 2019, **899**, 120908.
59 R. Verron, T. Achard, C. Seguin, S. Fournel and S. Bellemin-Laponnaz, *Eur. J. Inorg. Chem.*, 2020, **2020**, 2552–2557.
60 E. Chardon, G. Dahm, G. Guichard and S. Bellemin-Laponnaz, *Organometallics*, 2012, **31**, 7618–7621.
61 B. P. Maliszewski, I. Ritacco, M. Belis, I. I. Hashim, N. V. Tzouras, L. Caporaso, L. Cavallo, K. Van Hecke, F. Nahra, C. S. J. Cazin and S. P. Nolan, *Dalton Trans.*, 2022, **51**, 6204–6211.
62 M. Ameskal, R. Taakili, E. S. Gulyaeva, C. Duhayon, J. Willot, N. Lugan, C. Lepetit, D. A. Valyaev and Y. Canac, *Inorg. Chem.*, 2023, **62**, 20129–20141.
63 Y. Gao, C. Gesenberg and W. Zheng, in *Developing Solid Oral Dosage Forms*, ed. Y. Qiu, Y. Chen, G. G. Z. Zhang, L. Yu and R. V. Mantri, Academic Press, Boston, 2nd edn, 2017, pp. 455–495, DOI: **10.1016/B978-0-12-802447-8.00017-0**.
64 M. Bouche, A. Bonnefont, T. Achard and S. Bellemin-Laponnaz, *Dalton Trans.*, 2018, **47**, 11491–11502.
65 P. Papadia, F. Barozzi, J. D. Hoeschele, G. Piro, N. Margiotta and G. P. Di Sansebastiano, *Int. J. Mol. Sci.*, 2017, **18**, 306.
66 A. D. Bangham, M. W. Hill and N. G. A. Miller, *Preparation and use of liposomes as models of biological membranes*, 1974, ch. 1, pp. 1–68.
67 N. T. Huynh, C. Passirani, P. Saulnier and J. P. Benoit, *Int. J. Pharm.*, 2009, **379**, 201–209.
68 B. Heurtault, P. Saulnier, B. Pech, J. E. Proust and J. P. Benoit, *Pharm. Res.*, 2002, **19**, 875–880.
69 B. Campos, F. Wan, M. Farhadi, A. Ernst, F. Zeppernick, K. E. Tagscherer, R. Ahmadi, J. Lohr, C. Dictus, G. Gdynia, S. E. Combs, V. Goidts, B. M. Helmke, V. Eckstein, W. Roth, P. Beckhove, P. Lichter, A. Unterberg, B. Radlwimmer and C. Herold-Mende, *Clin. Cancer Res.*, 2010, **16**, 2715–2728.
70 D. Sehedic, I. Chourpa, C. Tetaud, A. Griveau, C. Loussouarn, S. Avril, C. Legendre, N. Lepareur, D. Wion, F. Hindre, F. Davodeau and E. Garcion, *Theranostics*, 2017, **7**, 4517–4536.
71 H. Lajous, R. Riva, B. Lelievre, C. Tetaud, S. Avril, F. Hindre, F. Boury, C. Jerome, P. Lecomte and E. Garcion, *Biomater. Sci.*, 2018, **6**, 2386–2409.
72 L. Roncali, S. Marionneau-Lambot, C. Roy, R. Eychenne, S. Gouard, S. Avril, N. Chouin, J. Riou, M. Allard, A. Rousseau, F. Guerard, F. Hindre, M. Cherel and E. Garcion, *EBioMedicine*, 2024, **105**, 105202.
73 M. J. Walters, K. Ebsworth, R. D. Berahovich, M. E. Penfold, S. C. Liu, R. Al Omran, M. Kioi, S. B. Chernikova, D. Tseng, E. E. Mulkearns-Hubert, M. Sinyuk, R. M. Ransohoff, J. D. Lathia, J. Karamchandani, H. E. Kohrt, P. Zhang, J. P. Powers, J. C. Jaen, T. J. Schall, M. Merchant, L. Recht and J. M. Brown, *Br. J. Cancer*, 2014, **110**, 1179–1188.
74 R. M. McQuade, V. Stojanovska, R. Stavely, C. Timpani, A. C. Petersen, R. Abalo, J. C. Bornstein, E. Rybalka and K. Nurgali, *Br. J. Pharmacol.*, 2018, **175**, 656–677.
75 W. F. Taylor and E. Jabbarzadeh, *Am. J. Cancer Res.*, 2017, **7**, 1588–1605.
76 L. Patrawala, T. Calhoun, R. Schneider-Broussard, J. Zhou, K. Claypool and D. G. Tang, *Cancer Res.*, 2005, **65**, 6207–6219.